



# Recycled polyethylene terephthalate/carbon nanotube composites with improved processability and performance

Ravindra Reddy Chowreddy<sup>1,\*</sup> , Katrin Nord-Varhaug<sup>1</sup> , and Florian Rapp<sup>2</sup> 

<sup>1</sup>Norner Research AS, Asdalstrand 291, 3962 Stathelle, Norway

<sup>2</sup>Fraunhofer Institute for Chemical Technology ICT, Joseph-von-Fraunhofer-Straße 7, 76327 Pfinztal, Germany

**Received:** 13 November 2017

**Accepted:** 8 January 2018

**Published online:**

17 January 2018

© Springer Science+Business Media, LLC, part of Springer Nature 2018

## ABSTRACT

Recycled poly(ethylene terephthalate) (PET) nanocomposites containing multi-walled carbon nanotubes (CNTs) were prepared through melt compounding via masterbatch dilution method. The masterbatch and the nanocomposites were processed in a twin-screw extruder. The rheological, morphological, thermal and mechanical properties of the PET–CNT nanocomposites have been investigated. Incorporation of CNTs into recycled PET at low concentration (0.25 wt%) significantly increases the viscosity. The storage modulus and loss modulus of nanocomposites were also increased with increasing amount of CNTs. This effect was more pronounced at lower frequencies. The incorporated CNTs in recycled PET increase the degree of crystallinity and crystallization temperature through heterogenous nucleation. Thermal stability and glass transition temperature of PET–CNT nanocomposites were slightly higher than the reference recycled PET. The tensile strength and modulus of PET–CNT nanocomposites increased even at low concentrations of CNTs. Morphological investigation through scanning electron microscopy indicated homogeneous dispersion of CNTs at lower concentrations. At higher concentrations, the CNTs tend to agglomerate due to nanotube–nanotube interactions.

## Introduction

Polymer nanocomposites (PNCs) containing organic and inorganic nanofillers have attracted great interest from both academia and industry due to their unique characteristics. PNCs exhibit superior mechanical properties, lower permeability for gases, improved flame retardancy, better thermal stability, improved

chemical resistance and enhanced thermal and electrical conductivity compared to neat polymers [1–7]. The enhanced properties of PNCs are due to incorporation of high strength, high aspect ratio and/or high surface area, and high surface reactivity of nanofillers into polymer matrix.

A wide variety of nanofillers such as clays, carbon nanotubes, graphene, cellulose and metal and

Address correspondence to E-mail: Ravindra.Chowreddy@norner.no

ceramics have been investigated in developing advanced PNCs. Carbon nanotubes (CNTs) are one of the most extensively investigated classes of nanofillers in developing advanced PNCs [1, 2]. The most widely used carbon nanotubes in PNCs are MWNTs due to their availability in large quantities and low cost. Fundamental research has shown that CNTs exhibit excellent mechanical properties, such as elastic modulus higher than 1.0 TPa and tensile strengths in the order of 10–60 GPa [8, 9]. In addition, CNTs possesses high electrical conductivity (in the range of  $10^7$ – $10^8$  S  $m^{-1}$ ) and high thermal conductivity (in the range from 2000 to 6000 W  $mK^{-1}$ ) [9]. These characteristics in addition to high surface area of CNTs suggest that the CNTs are potential functional nanofillers in developing advanced PNCs for range of applications [10–14].

One of the major challenges in developing high-performance PNCs has been obtaining a complete and homogeneous dispersion of CNTs in polymer matrix [15]. The incomplete and inhomogeneous dispersion of nanofillers leads to poor interfacial adhesion between nanofiller and polymer matrix and reduced performance of PNCs. However, good dispersion of CNTs in polymer matrix and high interfacial adhesion between CNTs and polymer matrix could be achieved by functionalization or surface modification of CNTs [16–19]. Any surface modification or functionalization of CNTs to improve interfacial adhesion in polymer nanocomposites leads to additional cost. In addition, the bottleneck for commercial exploitation of advanced PNCs has been their production in large scale in a reasonable low cost. Among three main processing techniques, solution, melt compounding and in situ polymerization, the melt compounding has been industrially accepted as a simple and efficient method as it produces PNCs in large scale at low costs [20]. Development of high-performance PNCs by combination of inexpensive thermoplastic matrix with small quantities of expensive CNTs with low manufacturing costs is of great interest [20, 21].

Although CNTs have been extensively investigated as reinforcement in a wide variety of polymers, investigations on compounds of CNT and recycled PET are scarce. Though there exist a few reports in the field of recycled PET–CNT nanocomposites [22, 23], none were focused in the direction of improving the performance of recycled PET. In the present communication, we are reporting the study

on recycled PET–CNT nanocomposites. The PET–CNT nanocomposites containing 0.25–1.0 wt% of CNTs were produced by conventional melt compounding using twin-screw extruder. The PET–CNT nanocomposites are investigated for rheological, thermal and mechanical properties.

## Materials and methods

### Materials

Recycled poly(ethylene terephthalate) (rPET), TEXPET R 760, was purchased from Texplast GmbH, Germany. The TEXPET R 760 was received in the form of pellets and was regranulate from the post-consumer PET bottles used in the beverage industry. The intrinsic viscosity (IV) of the material was  $0.80 \pm 0.02$  dL  $g^{-1}$ .

The carbon nanotubes (CNTs) utilized in the present study were Nanocyl<sup>®</sup> NC7000<sup>™</sup>, thin multi-walled carbon nanotubes from Nanocyl SA, Belgium. The Nanocyl<sup>®</sup> NC7000<sup>™</sup> were produced via the catalytic chemical vapour deposition (CCVD) process. The CNTs have the carbon purity of about 90%, average diameter 9.5 nm and average length of 1.5  $\mu$ m.

### Preparation of PET–CNT nanocomposites

The PET–CNT nanocomposites were processed via masterbatch dilution method. In this method, a PET–CNT masterbatch containing 10 wt% of carbon nanotubes (CNTs) was made first by melt compounding process. Later, the masterbatch was diluted with the neat resin by melt compounding to obtain a PET–CNT nanocomposite with appropriate CNT content. To produce masterbatch, the required amounts of milled recycled PET and CNTs are weighed, physically mixed well using kitchen blender and dried at 120 °C for overnight. Later, the mixture was melt-extruded using twin-screw Prism 24 extruder with  $L/D$  of 30. The extrusion was performed at 270 °C with the screw speed of 300 rpm. After compounding, the polymer string was cooled under water bath and pelletized.

In order to prepare PET–CNT nanocomposites, the required amounts of PET–CNT masterbatch and milled recycled PET (neat) material were weighed, physically mixed well and dried overnight at 120 °C.

Later, the dried mixture was melt-extruded using twin-screw Prism 16 extruder with  $L/D$  of 25. The extrusion was performed at 260 °C and the screw speed of 500 rpm. After compounding, the polymer string was cooled under water bath and pelletized. The PET–CNT nanocomposites containing 0.25, 0.50, 0.75 and 1.0 wt% CNTs was produced and are referred to as PET–CNT (0.25), PET–CNT (0.50), PET–CNT (0.75) and PET–CNT (1.0). The properties of PET strongly depend on its molecular weight. Melt processing of PET (in the presence of CNTs) could lead to a reduction in molecular weight due to mechanical stress due to shear forces in extruder and thermal or hydrolytic or oxidative degradation. For meaningful comparison of properties of the nanocomposites with reference PET, the neat recycled PET was also subjected to melt compounding under identical conditions as that for the PET–CNT nanocomposite preparation, and referred to as reference PET.

## Characterization of nanocomposites

### *Rheological measurements*

Dynamic rheological measurements on the PET–CNT nanocomposites were performed on Dynamic Analyser RDA II from Rheometric. The measurements were carried out with parallel plate flow geometry using 25-mm-diameter plates at 270 °C. Steady shear viscosity measurements were made in a shear rate range varying from 0.1 to 300  $\text{rad s}^{-1}$ . For rheological measurement, circular specimens with 30 mm diameter and 1.5 mm thickness were made by compression moulding. Before making the specimens by compression moulding, the PET–CNT nanocomposite pellets were dried well to avoid any degradation during compression moulding. The storage modulus, loss modulus and complex viscosity were measured.

### *Differential scanning calorimetry (DSC)*

Differential scanning calorimetry (DSC) analysis on PET–CNT nanocomposites was performed using Netzsch 204-F1 instrument. About 10–15 mg of pellet sample was encapsulated into sealed aluminium pans and analysed. The analysis involved three cycles of heating and cooling: (1) heating the sample from room temperature to 280 °C at a heating rate of 10 °C  $\text{min}^{-1}$  and held for 5 min, (2) cooling from 280

to 30 °C at a cooling rate of 10 °C  $\text{min}^{-1}$  and held for 5 min and (3) heating the sample from 30 to 280 °C at a heating rate of 10 °C  $\text{min}^{-1}$ . The glass transition temperature, melt temperature, crystallization temperature, crystallinity and enthalpies of melting and crystallization of PET–CNT nanocomposites were determined from DSC analysis.

### *Thermogravimetric analysis (TGA)*

Thermogravimetric analysis (TGA) on PET nanocomposite samples was carried out using Q500 from TA instruments. Thermograms obtained from TGA provide the information related to the thermal stability of material. About 10–15 mg of the sample was subjected to TGA. TGA was performed on the samples between room temperature and 750 °C with heating rate of 10 °C  $\text{min}^{-1}$  in both air and nitrogen atmospheres.

### *Dynamic mechanical analysis (DMA)*

Dynamic mechanical analysis (DMA) on PET–CNT nanocomposites was performed on DMA Q800 from TA Instruments using single cantilever in bending mode. Analysis was performed on bar-like cut specimens from compression-moulded plate. The specimen length, width and thickness, respectively, are 40, 5.0 and 2.0 mm. Experiments were performed between room temperature and 190 °C at the heating rate of 3 °C  $\text{min}^{-1}$ . The frequency of bending was fixed at 1 Hz. DMA was performed to evaluate the dynamic mechanical properties of nanocomposites and glass transition temperature.

### *Tensile testing*

Tensile testing on the PET–CNT nanocomposites was performed on Zwick Z010 according to ISO 527. Multipurpose type 1B injection-moulded dog-bone specimens were utilized for testing. The measurement was carried out at a cross-head rate of 5 mm  $\text{min}^{-1}$ . Five parallel measurements were made at room temperature, and average values are reported. Tensile properties such as tensile strength, modulus, elongation at yield and elongation at break were measured from the stress–strain curves.

### Gel permeation chromatography (GPC) analysis

Gel permeation chromatography (GPC) analysis on PET and nanocomposites provides the information about the average molecular weights,  $M_n$  and  $M_w$ , and the molecular weight distribution  $M_w/M_n$ . The GPC analysis was performed on Viscotek TDA 301 from Malvern. GPC analysis was performed on the samples using 1,1,1,3,3,3-hexafluoro-2-propanol (HFIP) as solvent. Chromatograms were obtained by using a refractive index detector, equipped with a PL HFIP gel guard plus 2× PL HFIP gel 300× 7.5 mm, 9 μm columns at a flow rate of 0.8 mL min<sup>-1</sup> and a nominal temperature of 40 °C. Poly(methyl methacrylate) (PMMA) was utilized to calibrate the GPC system and the results are expressed in “PMMA equivalent” molecular weights, suitable for comparative purpose among the samples.

### Scanning electron microscopy (SEM)

Scanning electron microscopic (SEM) investigation on nanocomposites was carried out using Philips XL-30 ESEM. For SEM analysis, a specimen was prepared by etching. First, a small piece of injection-moulded specimen was embedded into an epoxy resin and polished after curing. The polished specimen was exposed to 4 M aqueous potassium hydroxide (KOH) solution at around 80 °C to remove the surface PET resin by etching. The etched specimen was washed with water and dried, and a thin layer of gold was sputter-coated for SEM analysis. The SEM analysis was performed using secondary electron (SE) detector at an accelerating voltage of 30 kV.

## Results and discussion

### Processing of PET–CNT nanocomposites

During the processing of PET–CNT masterbatch, the temperature profile in the extrusion barrel was set flat at 270 °C from hopper to die. However, the temperature at middle of the extruder barrel to die was increased up to 300 °C. The increase in the temperature during the processing in the extrusion barrel indicates high shear forces and high viscosity build-up due to low-density CNTs. The increase in temperature in the extruder barrel was not observed

during the production of PET–CNT nanocomposites by dilution of masterbatch. These observations indicate no significant increase in the shear forces and the viscosity build-up in the extruder.

### Rheological measurements

Rheological characterization is often carried out on the polymer nanocomposite samples to obtain qualitative information related to nanofiller dispersion and percolation threshold of nanofiller in the resin. The rheological properties of nanocomposite melt are sensitive to structure, particle size, shape and interfacial properties of dispersed phase in the resin and hence the dispersion quality [24].

Variation of complex viscosity of the reference PET and the PET–CNT nanocomposites as a function of frequency is presented in Fig. 1a. It is clear from the complex viscosity plots that the viscosity of neat PET is independent of frequency indicating Newtonian behaviour. The nanocomposite containing 0.25 wt% CNTs, PET–CNT (0.25) showed weak shear thinning behaviour. However, nanocomposite samples containing 0.50 wt% and above exhibited a pronounced shear thinning response. The shear thinning effect in PET nanocomposites increases with the increase in CNT loading. Further, increase in the viscosity was observed for PET nanocomposites with the increase in CNT loading and which was more pronounced at low frequency. The reduced viscosity at higher frequency is due to the shear thinning effect. The observed results are in good agreement with the literature [21, 25, 26].

The variation of storage modulus ( $G'$ ) of reference PET and PET–CNT nanocomposites as a function of frequency is presented in Fig. 1b. The storage modulus of the PET–CNT nanocomposites increases with CNT loading. The storage modulus of PET–CNT nanocomposites increases significantly compared to the reference PET, especially in the low-frequency range. An increase in storage modulus means a more elastic structure, which indicates the restriction of polymer chain motion due to the CNT fillers [27]. Further, the storage modulus of reference PET and PET–CNT nanocomposites increases with the increase in the frequency. The magnitude of storage modulus increase with frequency is higher for reference PET and PET–CNT (0.25) compared to other nanocomposites. The dependence of storage modulus on frequency for PET–CNT (0.25) is similar to that of



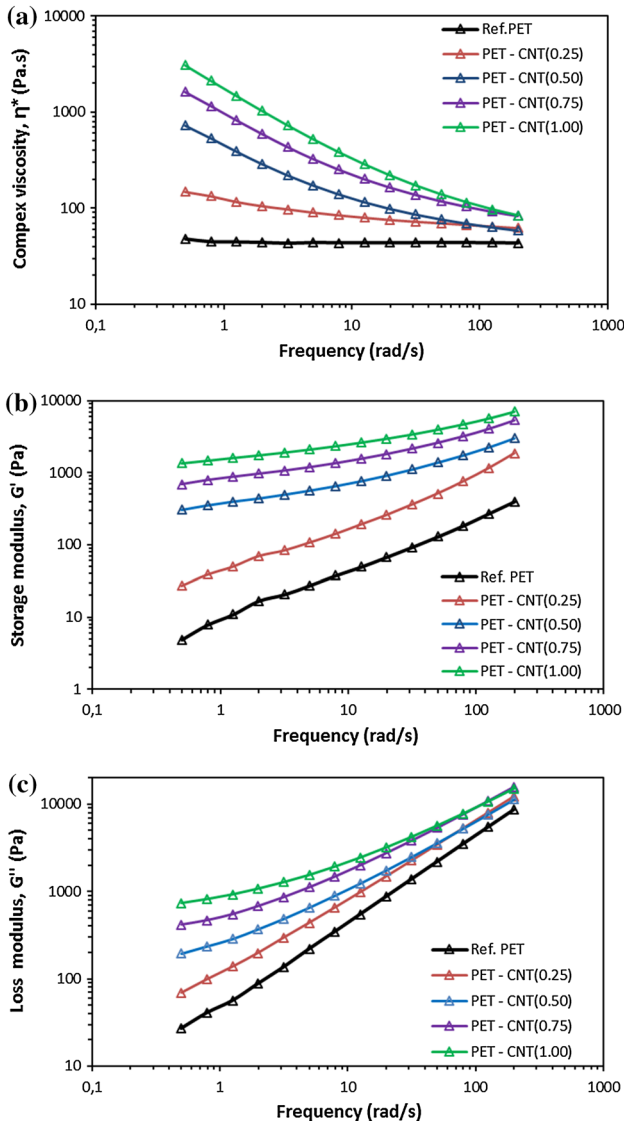


**Figure 1** Variation of **a** complex viscosity, **b** storage modulus and **c** loss modulus of PET and PET–CNT nanocomposites, at 270 °C and 10% strain rate.

the neat PET material, indicating both the samples possess similar viscoelastic properties. However, for PET–CNT nanocomposites with CNT loading 0.50% and above, there is a less pronounced dependency of storage modulus on frequency and storage modulus curves exhibit a plateau at the lowest frequencies (Fig. 1b). The observed plateau behaviour at lower frequency for PET–CNT nanocomposites is attributed to interconnected or network structures due to nanotube–nanotube (solid–solid) and nanotube–polymer (solid–polymer) interactions [21, 25, 28]. Such interconnected or network structures between nanotubes and with resin indicate the percolation network.

Similar observations are reported in the literature for other polymer composites [26, 29, 30].

The variation of loss modulus ( $G''$ ) of the reference PET and PET–CNT nanocomposites as a function of frequency is presented in Fig. 1c. The trend in the variation of loss modulus with frequency for nanocomposites is similar to that of the storage modulus (Fig. 1b); however, the increase in loss modulus with the increase in CNT content is not very significant. The increase in loss modulus means that the viscous behaviour increases with added CNTs. The CNTs present in matrix act as cross-linking agents and reduces the molecular motion and hence increased viscous response.

### DSC analysis results

Thermal properties and crystallization behaviour of the reference PET and nanocomposites were investigated by using differential scanning calorimetry (DSC). The results DSC analysis, crystallization temperatures ( $T_c$ ), melting temperatures ( $T_m$ ), enthalpies of crystallization and melting ( $\Delta H_c$  and  $\Delta H_m$ ) and degree of crystallinity are presented in Table 1. The degree of crystallinity ( $X_c$ ) was determined from the melting enthalpy values using following equation:

$$X_c = \frac{\Delta H_m}{(1 - \phi)\Delta H_m^o} \times 100$$

where  $\Delta H_m$  is second melting enthalpy of the samples ( $J g^{-1}$ ),  $\Delta H_m^o$  is the enthalpy value of melting of a 100% crystalline form of PET,  $117.6 J g^{-1}$  [31], and  $\phi$  is the weight fraction of filler.

It is clear from the results that the incorporation of CNTs into the PET matrix has very little influence on melting temperature,  $T_m$  of nanocomposite samples. However, incorporation of CNTs into PET increases the crystallization temperature ( $T_c$ ) of nanocomposites. The  $T_c$  of the nanocomposite with lowest CNT content (PET–CNT (0.25)) is 13 °C higher than the  $T_c$  of the reference. The nanocomposites containing higher amounts of CNTs, 0.5 wt% and above presented slightly higher  $T_c$  compared to the PET–CNT (0.25). In addition, the degree of crystallinity calculated for the PET–CNT nanocomposites slightly increases with the increase in CNT content. The increase in crystallization temperature and the degree of crystallinity in PET–CNT nanocomposites is due to the nucleation effect of CNTs in the PET matrix. The presence of nanoreinforcements, such as clays and

**Table 1** Results of DSC analysis— $T_m$ ,  $T_c$ , enthalpy of melting, degree of crystallinity and  $\Delta T$ 

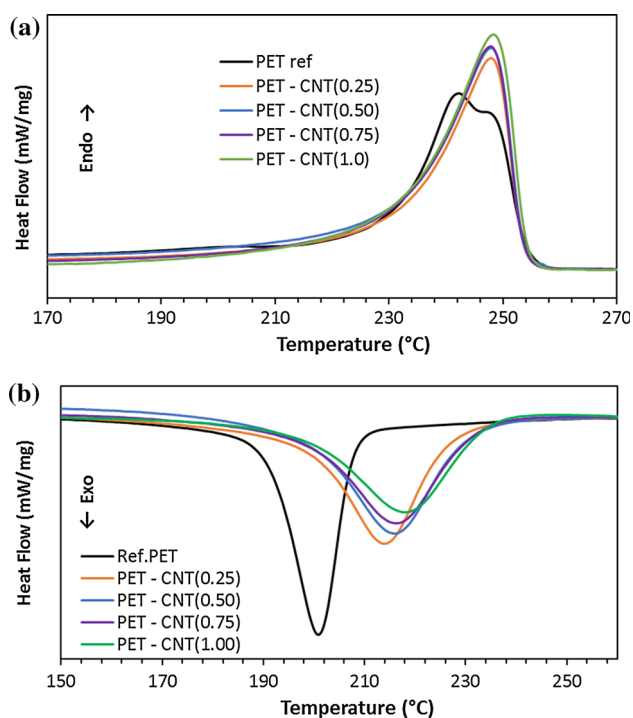
Sample	$T_m$ (°C)	$T_c$ (°C)	Enthalpy of melting ( $J g^{-1}$ )	Crystallinity (%)	$\Delta T = T_m - T_c$ (°C)
Ref. PET	247	201	41	34.9	46
PET–CNT (0.25)	248	214	41	34.9	34
PET–CNT (0.50)	248	216	45	38.3	32
PET–CNT (0.75)	248	216	43	36.6	32
PET–CNT (1.00)	248	218	47	40.0	30

CNTs, are known to exhibit nucleating effect in polymer matrices [3, 32, 33]. The degree of supercooling,  $\Delta T$ , is seen to slightly decrease with the increase in the CNT content (Table 1). The results indicate that the incorporation of CNTs at as low as 0.25 wt% loading effectively enhances the crystallization of PET matrix through heterogeneous nucleation. Similar observations are made in the literature [21].

The DSC thermograms, second heating curve and cooling curve, for reference PET and nanocomposites are presented in Fig. 2. It can be noticed from the second heating curves (Fig. 2a) that the reference PET material presented a double melting peak. The double melting peaks in PET could be due the presence of dual lamella thickness distribution produced

during crystallization [34]. The PET–CNT composites present only a single melting peak meaning that the incorporation of CNTs into PET matrix alters the crystallization behaviour. The presence of CNTs in recycled PET matrix induces the homogeneous crystal growth and structure. The position of melting endotherm for all the composite samples was not altered.

The DSC crystallization endotherms of PET and PET–CNT nanocomposites are presented in Fig. 2b. It is clearly observed from the crystallization endotherms that the nanocomposite materials crystallize at higher temperatures compared to reference PET, as also seen from the corresponding  $T_c$  values in Table 1. It can be noticed from the results that the incorporation of CNTs at 0.25 wt% loading in PET increases the  $T_c$  by 13 °C compared to the reference PET. With the increase in CNT content in PET matrix, the crystallization temperature of nanocomposites is increased slightly due to nucleating affinity of the added CNTs. Similar observations are made in the literature [35].

**Figure 2** DSC melting endotherms (a) and crystallization exotherms (b) for reference PET and PET–CNT nanocomposites.

### TGA results

It has been reported in the literature that the incorporation of CNTs into polymers enhances the thermal stability [36–38]. To investigate the thermal stability of the PET–CNT nanocomposites, thermogravimetric analysis (TGA) was performed. The TGA was performed under both nitrogen and air atmospheres. The TGA of samples analysed under nitrogen and air atmospheres, respectively, represent the pyrolytic and thermo-oxidative conditions. The TGA weight loss curves and first derivative TGA curves for reference PET and the nanocomposite samples analysed under air atmosphere are presented in Fig. 3. Figure 3 shows that the samples exhibiting two-step decomposition during TGA under air, an oxidative environment. The first step of

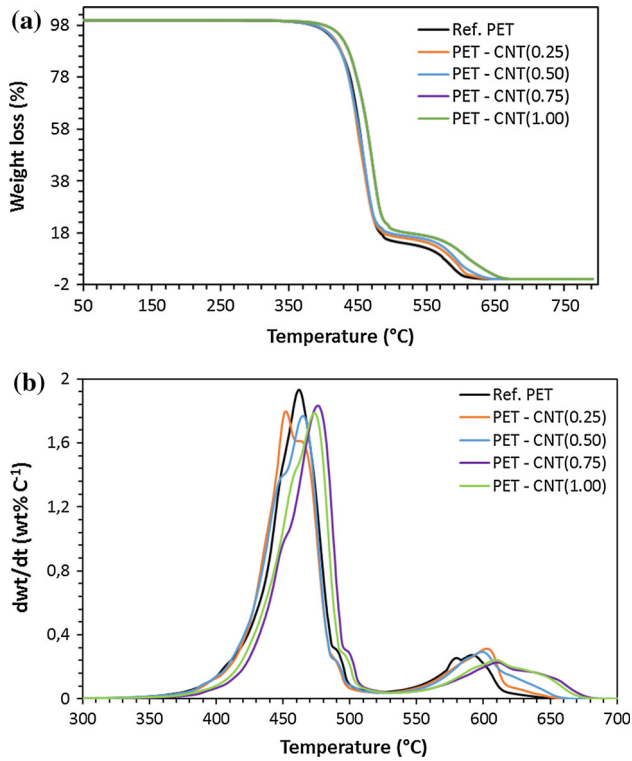


**Figure 3** **a** TGA weight loss curves and **b** first derivative TGA curves for reference PET and nanocomposites during TGA under air atmosphere.

decomposition for PET is due to overlap of two decomposition processes: the first process is mainly due to the degradation of polymer chain through end group-initiated mechanism and the second process is due to the thermal degradation of the products formed during first decomposition process [39]. The second degradation step for PET, in the temperature range 520–640 °C, is due to the decomposition of thermally stable species such as cross-linked carbonaceous structures formed during the first degradation step. The PET–CNT nanocomposites presented similar weight loss/thermal degradation behaviour except a small shift in the degradation temperature to a slightly higher temperature. The improvement in thermal stability is not very large. The improved thermal stability in PET–CNT nanocomposites could be due to the physical barrier action of dispersed CNTs for transport of volatile decomposed products during thermal decomposition [19].

The TGA weight loss curves and first derivative TGA curves for reference PET and the nanocomposite samples analysed under nitrogen atmosphere,

pyrolytic environment are presented in Fig. 4. Unlike, TGA under air atmosphere, both the reference PET and nanocomposites exhibited one-step decomposition during the TGA under nitrogen atmosphere. The main degradation process during TGA under nitrogen is due to the combined degradation processes—polymer chain degradation through end group-initiated mechanism and the thermal degradation of the products formed during polymer chain degradation process. Both PET and its nanocomposites presented almost similar weight loss behaviour and hence similar thermal stability. Under nitrogen environment, the thermal decomposition of polymer is also leading to the thermally stable cross-linked carbonaceous species which are not undergoing any further decomposition due to the presence of inert nitrogen atmosphere and hence the large amounts of residue at the end of the TGA.

The results of TGA such as temperature at 1% weight loss, temperature at 5% weight loss, onset of decomposition and the amount of residue at end of TGA (at 750 °C) are summarized in Table 2. It is clear from the results that the nanocomposite samples

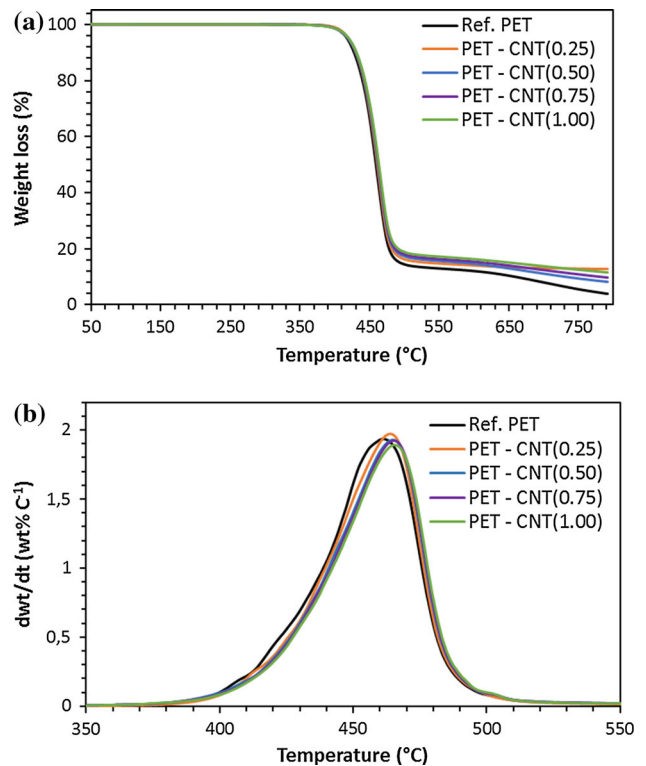


**Figure 4** **a** TGA weight loss curves and **b** first derivative TGA curves for reference PET and nanocomposites during TGA under nitrogen atmosphere.

**Table 2** Results of TGA

Sample	Temp. at 1% weight loss		Temp. at 5% weight loss		Onset of decomposition		Weight loss during second decomposition (%)		Residual mass at 750 °C (%)	
	Air	N <sub>2</sub>	Air	N <sub>2</sub>	Air	N <sub>2</sub>	Air	N <sub>2</sub>	Air	N <sub>2</sub>
Ref. PET	366	396	406	416	429	432	13.8	NA	0.2	4.5
PET–CNT (0.25)	369	397	406	418	430	432	16.0	NA	0.2	8.0
PET–CNT (0.50)	371	397	407	420	428	437	16.8	NA	0.2	9.5
PET–CNT (0.75)	386	395	421	421	441	438	17.5	NA	0.3	11.5
PET–CNT (1.00)	380	394	417	421	437	438	17.9	NA	0.3	12.6

exhibited slightly higher temperature for 1% weight loss, 5% weight loss and onset of decomposition compared to reference PET material under air atmosphere. However, the PET and nanocomposites presented almost similar decomposition temperatures. The amount of residue left over on TGA (at 750 °C) under nitrogen atmosphere is higher than that of the TGA under air atmosphere.

### DMA results

Dynamic mechanical analysis (DMA) was carried out on neat PET and PET–CNT nanocomposites in order to understand the viscoelastic behaviour of the materials. The DMA measurements on PNCs provide information related to the influence of incorporated reinforcements on the polymer mobility. As a general trend, homogeneous incorporation of nanofillers into polymers leads to improved mechanical properties. However, inhomogeneous incorporation (agglomeration) of nanofillers into polymers leads to inferior mechanical properties due to introduction of weak points or defects in polymer by agglomerated fillers. Variation of storage modulus, loss modulus and  $\tan \delta$  with temperature for PET–CNT nanocomposites is presented in Fig. 5, respectively.

The effect of incorporation of CNTs on storage modulus of PET with temperature is presented in Fig. 5a. The DMA data, such as storage modulus at 30 and 80 °C and glass transition measured from maxima of loss modulus, are presented in Table 3. It is clear from the results that the PET–CNT nanocomposites exhibited higher storage modulus than reference PET throughout the measured temperature range. PET–CNT (0.25) obtained 13% increases in storage modulus at 30 °C compared to the reference PET. With the increase in the CNTs loading in PET

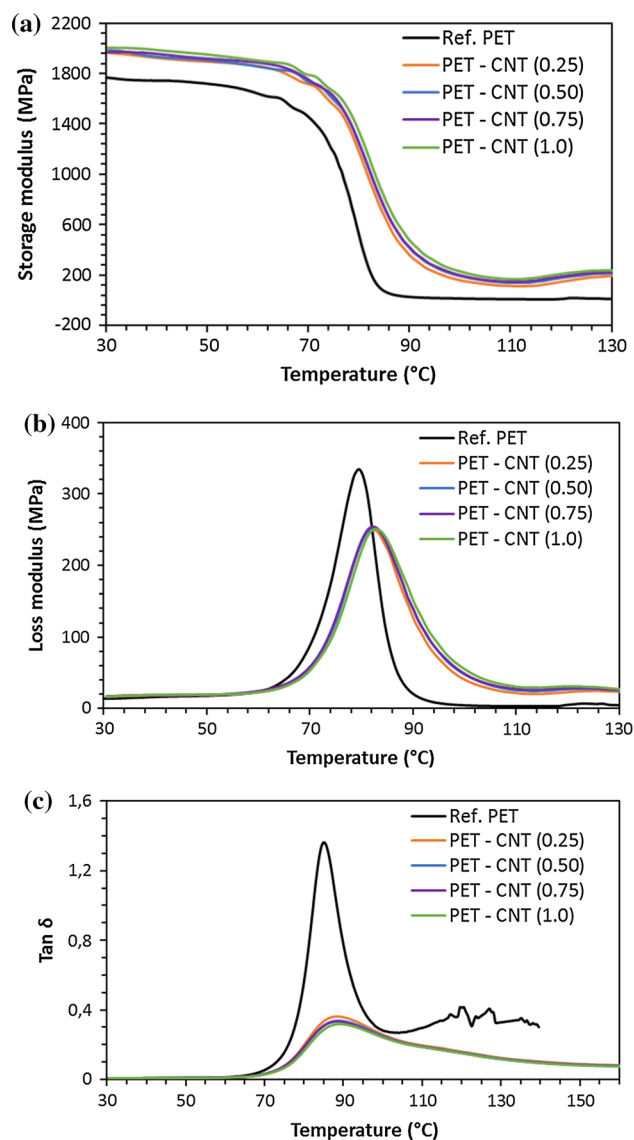


**Figure 5** Variation of storage modulus (a), loss modulus (b) and  $\tan \delta$  (c) with temperature for reference PET and PET–CNT nanocomposites.



**Table 3** Values of storage modulus at 30 and 80 °C, and  $T_g$  from DMA

Sample	Storage modulus at 30 °C (MPa)	Storage modulus at 80 °C (MPa)	Glass transition temperature, $T_g$ (°C)
Ref. PET	1742	617	81
PET–CNT (0.25)	1965	1240	82
PET–CNT (0.50)	1986	1239	82
PET–CNT (0.75)	1999	1288	83
PET–CNT (1.00)	2010	1300	83

samples, there was a further minor increase in storage modulus. The improved storage modulus in PET–CNT nanocomposites is due to the reinforcement effect of CNTs in the PET. The PET–CNT nanocomposites containing different amounts of CNTs presented similar storage modulus curves throughout the measured temperature range. From the DMA plots, a rapid decrease in the moduli was observed at around 80 °C after a slow decrease in moduli in lower-temperature region. The glass transition temperature at around 80 °C is not very much influenced by the added CNTs. The storage modulus of PET–CNT nanocomposites at 80 °C is almost 100% higher than that of reference PET sample, indicating higher thermal stability of PET–CNT nanocomposites.

Variation of loss modulus for the reference PET and PET–CNT nanocomposites is presented in Fig. 5b. The glass transition  $T_g$  values of materials were calculated based on the temperature maxima in loss modulus curves and are presented in Table 3. The  $T_g$  of PET–CNT nanocomposites is slightly higher than the reference PET sample and increased slightly with the increase in CNT loading. However, the increase in  $T_g$  is not significant. The effect of incorporated CNTs on  $T_g$  of thermoplastics is not well understood, as both increase and decrease of  $T_g$  is reported in the literature.

Tan  $\delta$  represents the viscous to elastic response of viscoelastic material. The tan  $\delta$  curves as a function of temperature for reference PET and PET–CNT nanocomposites are presented in Fig. 5c. It is clear from the plots that the tan  $\delta$  values for PET–CNT nanocomposites are lower than the neat PET material indicating that the PET–CNT nanocomposite presents more elastic response. There was no significant difference between the tan  $\delta$  curves for the various PET–CNT nanocomposites.

## GPC analysis results

The properties of PET strongly depend on its molecular weight. Melt processing of PET could lead to a reduction in molecular weight due to thermal or hydrolytic or oxidative degradation during melt processing. For meaningful comparison of properties among the PET–CNT nanocomposites, the molecular weight of PET was determined by GPC analysis. The results of GPC analysis, weight average molecular weight  $M_w$ , the number average molecular weight  $M_n$  and the molecular weight distribution  $M_w/M_n$  for reference PET and PET–CNT nanocomposites are presented in Table 4. The reference PET and PET–CNT nanocomposites showed slightly lower molecular weights compared to the as received PET material. The reference material and PET–CNT nanocomposites have undergone extrusion processing, and the materials are therefore expected to present reduction in molecular weight due to thermal degradation. There is no significant difference in molecular weight between reference PET and nanocomposites, indicating that the presence of CNTs during thermal processing has no influence on degradation of PET.

**Table 4** GPC analysis results of PET and PET–CNT nanocomposites

Sample	$M_w$	$M_n$	$M_w/M_n$
As received PET	34350	7460	4.6
Ref. PET	30550	9065	3.4
PET–CNT (0.25)	31650	8855	3.6
PET–CNT (0.50)	30450	7665	4.0
PET–CNT (0.75)	30450	8840	3.4
PET–CNT (1.00)	30050	8760	3.4

## Tensile properties

Typical stress–strain curves of reference PET and the PET–CNT nanocomposites containing different amounts of CNTs are presented in Fig. 6. Reference PET (unfilled) presented the characteristic extensive deformation after yielding. Inclusion of CNTs into PET increases the elongation at break. The reason is that the added CNTs in the PET matrix behave like physical or chemical cross-linking agents and restrict the moment of polymer chains [40].

The variations of the tensile strength and tensile modulus of the PET–CNT nanocomposites are presented in Fig. 7a. It is clear from the results that incorporation of CNTs into PET increases the tensile strength and modulus. The PET nanocomposite sample containing 0.25 wt% CNTs attained significant increase in tensile strength and modulus compared to reference PET matrix. The enhancement in tensile strength and modulus in PET–CNT nanocomposite is attributed to the reinforcement effect of homogeneously dispersed high aspect ratio of CNTs in PET matrix. However, with higher loading of CNTs in the nanocomposite, the further increase in strength and modulus was more modest. The modest increase in tensile strength and modulus in nanocomposites with CNT content could be due to the agglomeration of CNTs at higher concentrations. At higher concentration, the individual CNTs are known to agglomerate due to intrinsic van der Waals interactions, preventing efficient load transfer to the polymer matrix [21].

Variation of elongation at yield and elongation at break for reference PET and PET nanocomposites is

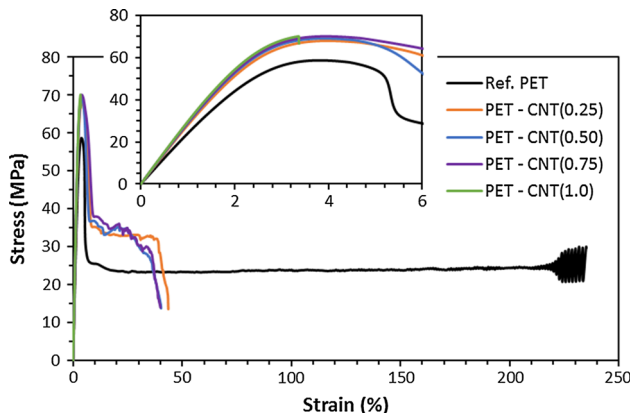


**Figure 6** Typical stress–strain curves of reference PET and PET–CNT nanocomposites.

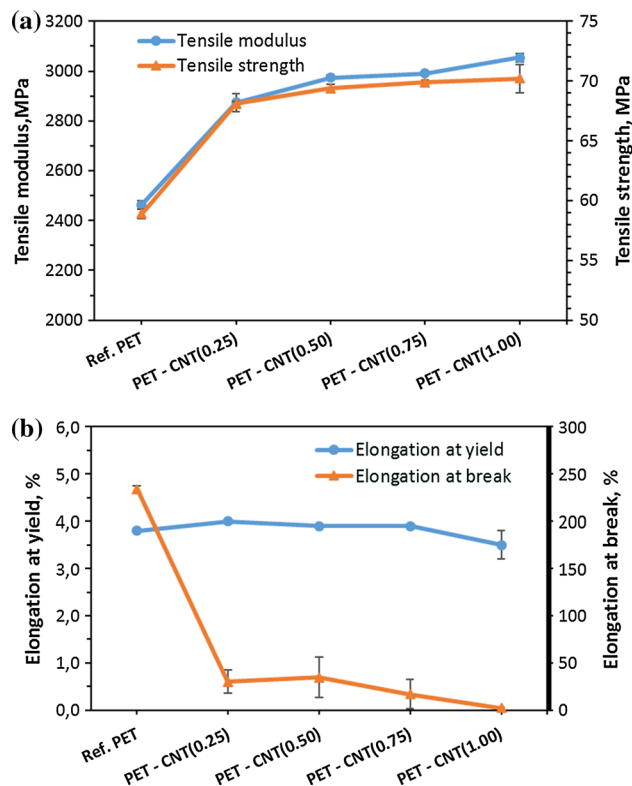


**Figure 7** Tensile strength and tensile modulus (a) and elongation at yield and elongation at break for of PET–CNT nanocomposites (b).

presented in Fig. 7b. Elongation at yield for both reference PET and PET–CNT nanocomposites was in the same order and varied between 3.5 and 4.0%. The elongation at break for reference PET was in the order of 230% and was reduced to 30, 35, 17 and 3%, respectively, for PET–CNT (0.25), PET–CNT (0.5), PET–CNT (0.75) and PET–CNT (1.0). The reduction in elongation at break for nanocomposites compared to reference PET is significant.

## Morphological results

SEM analysis was performed on the etched surfaces of injection-moulded specimens, and the resulting images are presented in Fig. 8. Composite material at lower loading, 0.25 wt%, presented a reasonable uniform dispersion of CNTs with relatively low agglomeration. With a higher loading of CNTs, some agglomeration and entanglement were observed. The agglomerated CNTs were, however, evenly distributed in the PET matrix. It is well known from the literature that at higher concentrations of CNTs they tend to self-agglomerate and form highly

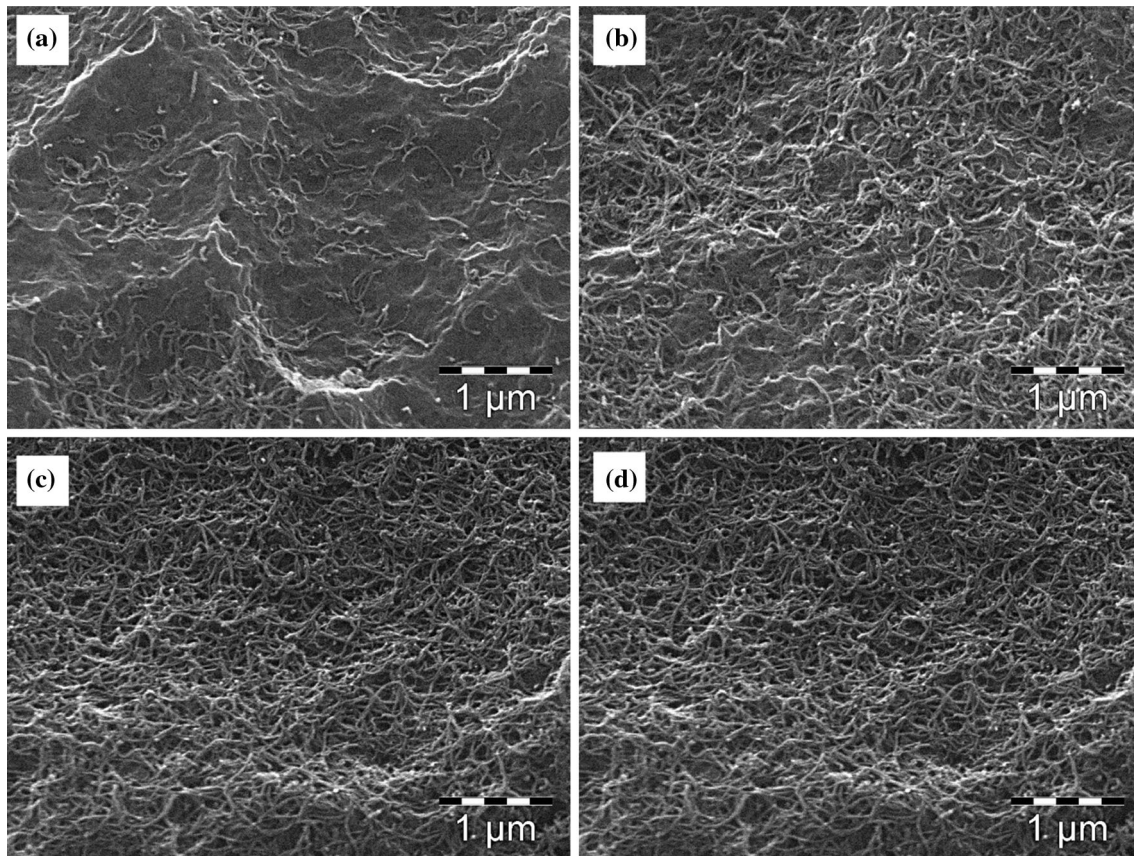


**Figure 8** SEM images of PET–CNT (0.25) (a), PET–CNT (0.50) (b), PET–CNT (0.75) (c) and PET–CNT (1.00) (d) at magnification of  $\times 25000$ .

interconnected or network structures [41, 42]. The highly agglomerated structures of CNTs in nanocomposite can act as weak points and could reduce the mechanical performance. From the morphological investigations, it can be concluded that the optimal concentration of CNTs in PET–CNT nanocomposites is around 0.25 wt%.

## Conclusion

The complex viscosity, storage modulus and loss modulus of PET–CNT nanocomposites were increased with addition of CNTs. The rheological results indicated that the percolation threshold, where nanotube–nanotube interaction is dominant, is about 0.50 wt%. The incorporated CNTs in recycled PET act as heterogeneous nucleating agents, resulting in an increase in the degree of crystallinity and crystallization temperature. Incorporation of CNTs into recycled PET slightly improves the thermal stability and glass transition temperature. A reinforcing

effect was seen on tensile strength and tensile modulus by as low as 0.25 wt% CNT in the nanocomposites. At higher CNT concentration, nanotube–nanotube interactions are dominant leading to an agglomerate or network structure of CNTs. The morphological investigation by scanning electron microscopy indicated homogeneous dispersion of CNTs at lower concentrations, whereas at higher concentrations, network structures of CNTs with higher degree of entangled were observed.

The incorporation of CNTs into recycled PET increases the viscosity and improves the thermal and mechanical properties. These improved properties make the material suitable for extrusion and injection moulding applications. For recycled PET, it is beneficial to increase the viscosity and the possible applications for recycled PET–CNT nanocomposites are industrial sectors where the improved properties such as strength and thermal stability can be utilized.



## Acknowledgements

The research leading to these results has received funding from the European Union's Seventh Framework Programme (FP7) under Grant Agreement No. 309985. The authors would like to thank the Smithers Rapra, UK, for their support with GPC analysis on the samples.

## References

- [1] Byrne MT, Gun'ko YK (2010) Recent advances in research on carbon nanotube–polymer composites. *Adv Mater* 22:1672–1688
- [2] Moniruzzaman M, Winey KI (2006) Polymer nanocomposites containing carbon nanotubes. *Macromolecules* 39:5194–5205
- [3] Paul D, Robeson LM (2008) Polymer nanotechnology: nanocomposites. *Polymer* 49:3187–3204
- [4] Okada A, Usuki A (2006) Twenty years of polymer–clay nanocomposites. *Macromol Mater Eng* 291:1449–1476
- [5] Kim H, Abdala AA, Macosko CW (2010) Graphene/polymer nanocomposites. *Macromolecules* 43:6515–6530
- [6] Siró I, Plackett D (2010) Microfibrillated cellulose and new nanocomposite materials: a review. *Cellulose* 17:459–494
- [7] Zaman I, Manshoor B, Khalid A, Araby S (2014) From clay to graphene for polymer nanocomposites—a survey. *J Polym Res* 21:429–439
- [8] De Volder MF, Tawfick SH, Baughman RH, Hart AJ (2013) Carbon nanotubes: present and future commercial applications. *Science* 339:535–539
- [9] Mittal G, Dhand V, Rhee KY, Park S-J, Lee WR (2015) A review on carbon nanotubes and graphene as fillers in reinforced polymer nanocomposites. *J Ind Eng Chem* 21:11–25
- [10] Dalton AB, Collins S, Munoz E, Razal JM, Ebron VH, Ferraris JP et al (2003) Super-tough carbon-nanotube fibres. *Nature* 423:703
- [11] Ishihara T, Kawahara A, Nishiguchi H, Yoshio M, Takita Y (2001) Effects of synthesis condition of graphitic nanocarbon tube on anodic property of Li-ion rechargeable battery. *J Power Sources* 97:129–132
- [12] Fan S, Chapline MG, Franklin NR, Tomblor TW, Cassell AM, Dai H (1999) Self-oriented regular arrays of carbon nanotubes and their field emission properties. *Science* 283:512–514
- [13] Kong J, Franklin NR, Zhou C, Chapline MG, Peng S, Cho K et al (2000) Nanotube molecular wires as chemical sensors. *Science* 287:622–625
- [14] Liu C, Fan Y, Liu M, Cong H, Cheng H, Dresselhaus MS (1999) Hydrogen storage in single-walled carbon nanotubes at room temperature. *Science* 286:1127–1129
- [15] Peponi L, Puglia D, Torre L, Valentini L, Kenny JM (2014) Processing of nanostructured polymers and advanced polymeric based nanocomposites. *Mater Sci Eng R Rep* 85:1–46
- [16] Wang C, Guo Z-X, Fu S, Wu W, Zhu D (2004) Polymers containing fullerene or carbon nanotube structures. *Prog Polym Sci* 29:1079–1141
- [17] Hirsch A (2002) Functionalization of single-walled carbon nanotubes. *Angew Chem Int Ed* 41:1853–1859
- [18] Bellayer S, Gilman JW, Eidelman N, Bourbigot S, Flambard X, Fox DM et al (2005) Preparation of homogeneously dispersed multiwalled carbon nanotube/polystyrene nanocomposites via melt extrusion using trialkyl imidazolium compatibilizer. *Adv Funct Mater* 15:910–916
- [19] Kim JY, Choi HJ, Kang CS, Kim SH (2010) Influence of modified carbon nanotube on physical properties and crystallization behavior of poly(ethylene terephthalate) nanocomposite. *Polym Compos* 31:858–869
- [20] Kim JY, Kim SH (2012) High performance PET/carbon nanotube nanocomposites: preparation, characterization, properties and applications. In: *Nanocomposites—new trends and developments*. InTech
- [21] Kim JY, Park HS, Kim SH (2007) Multiwall-carbon-nanotube-reinforced poly(ethylene terephthalate) nanocomposites by melt compounding. *J Appl Polym Sci* 103:1450–1457
- [22] Mallakpour S, Behranvand V (2017) Application of recycled PET/carboxylated multi-walled carbon nanotube composites for Cd<sup>2+</sup> adsorption from aqueous solution: a study of morphology, thermal stability, and electrical conductivity. *Colloid Polym Sci* 295:453–462
- [23] Mallakpour S, Behranvand V (2016) Manufacture and characterization of nanocomposite materials obtained from incorporation of D-glucose functionalized MWCNTs into the recycled poly(ethylene terephthalate). *Des Monomers Polym* 19:283–289
- [24] Hejazi I, Seyfi J, Sadeghi GMM, Davachi SM (2011) Assessment of rheological and mechanical properties of nanostructured materials based on thermoplastic olefin blend and organoclay. *Mater Des* 32:649–655
- [25] Hu G, Zhao C, Zhang S, Yang M, Wang Z (2006) Low percolation thresholds of electrical conductivity and rheology in poly(ethylene terephthalate) through the networks of multi-walled carbon nanotubes. *Polymer* 47:480–488
- [26] Seo M-K, Park S-J (2004) Electrical resistivity and rheological behaviors of carbon nanotubes-filled polypropylene composites. *Chem Phys Lett* 395:44–48



- [27] Bai J, Goodridge RD, Hague RJ, Song M, Okamoto M (2014) Influence of carbon nanotubes on the rheology and dynamic mechanical properties of polyamide-12 for laser sintering. *Polym Test* 36:95–100
- [28] Gupta A, Choudhary V (2013) Rheologic and mechanical properties of multiwalled carbon nanotubes-reinforced poly(trimethylene terephthalate) composites. *J Mater Sci* 48:3347–3356. <https://doi.org/10.1007/s10853-012-7025-7>
- [29] Wu D, Zhou C, Hong Z, Mao D, Bian Z (2005) Study on rheological behaviour of poly(butylene terephthalate)/montmorillonite nanocomposites. *Eur Polym J* 41:2199–2207
- [30] Du F, Scogna RC, Zhou W, Brand S, Fischer JE, Winey KI (2004) Nanotube networks in polymer nanocomposites: rheology and electrical conductivity. *Macromolecules* 37:9048–9055
- [31] Imai Y, Inukai Y, Tateyama H (2003) Properties of poly(ethylene terephthalate)/layered silicate nanocomposites prepared by two-step polymerization procedure. *Polym J Tokyo* 35:230–235
- [32] Ou CF, Ho MT, Lin JR (2003) The nucleating effect of montmorillonite on crystallization of PET/montmorillonite nanocomposite. *J Polym Res* 10:127–132
- [33] Manchado ML, Valentini L, Biagiotti J, Kenny J (2005) Thermal and mechanical properties of single-walled carbon nanotubes–polypropylene composites prepared by melt processing. *Carbon* 43:1499–1505
- [34] Kong Y, Hay J (2003) Multiple melting behaviour of poly(ethylene terephthalate). *Polymer* 44:623–633
- [35] Anand KA, Agarwal U, Joseph R (2006) Carbon nanotubes induced crystallization of poly(ethylene terephthalate). *Polymer* 47:3976–3980
- [36] Ou CF (2003) Nanocomposites of poly(trimethylene terephthalate) with organoclay. *J Appl Polym Sci* 89:3315–3322
- [37] Park C, Ounaies Z, Watson KA, Crooks RE, Smith J, Lowther SE et al (2002) Dispersion of single wall carbon nanotubes by in situ polymerization under sonication. *Chem Phys Lett* 364:303–308
- [38] Corcione CE, Frigione M (2012) Characterization of nanocomposites by thermal analysis. *Materials* 5:2960–2980
- [39] Wang X-S, Li X-G, Yan D (2000) Thermal decomposition kinetics of poly(trimethylene terephthalate). *Polym Degrad Stab* 69:361–372
- [40] Jin SH, Park Y-B, Yoon KH (2007) Rheological and mechanical properties of surface modified multi-walled carbon nanotube-filled PET composite. *Compos Sci Technol* 67:3434–3441
- [41] Wong M, Paramsothy M, Xu X, Ren Y, Li S, Liao K (2003) Physical interactions at carbon nanotube–polymer interface. *Polymer* 44:7757–7764
- [42] Frankland S, Harik VM (2003) Analysis of carbon nanotube pull-out from a polymer matrix. *Surf Sci* 525:L103–L108